

# AURORAL ABSORPTION OF COSMIC RADIO NOISE

By R. H. EATHER\* and F. JACKA†

[Manuscript received October 11, 1965]

## Summary

Inconsistencies in previous work on the association of auroras with ionospheric absorption of cosmic radio noise are discussed and attributed to a number of experimental factors.

Such "auroral absorption" events observed at the Australian National Antarctic Research Expeditions station at Mawson may be classified into four types: (i) day-time events, (ii) weak night-time ionospheric absorption, (iii) sudden ionospheric absorption (SIA), (iv) slowly varying ionospheric absorption (SVIA). During SIA events, peaks of absorption and auroral ( $\lambda 5577$ ) intensity are simultaneous and the absorption is limited to the luminous regions of the sky. During SVIA events, the absorption is more widespread and there is little correlation between absorption fluctuations and auroral intensity fluctuations; the ratio of absorption to intensity may be of the order of 100 times greater than in SIA events.

The variation observed in the absorption/intensity ratio from event to event, and within single events, is attributed to changes in the incident electron energy spectrum. Spectra varying as  $\exp(-\epsilon/\beta)$  are considered and a range in  $\beta$  from 5 to 24 keV is required to explain SIA events; this is in good agreement with rocket data. Consideration of the day/night ratio, two-frequency measurements, and simultaneity of auroral intensity and riometer absorption leads to a lower limit to the height of the absorbing region varying from 80 to 95 km, depending on the electron energy spectrum.

Comparison of riometer and  $H\beta$  photometer records suggests that protons are important in explaining SVIA events and could in fact be solely responsible.

## I. INTRODUCTION

The problems associated with the auroral absorption of cosmic radio noise have received much attention since the introduction of the riometer in 1959 (Little and Leinbach 1959). Although a considerable amount of experimental data has now been collected, there is still disagreement over the questions of:

- (a) the simultaneity of occurrence of absorption and aurora,
- (b) the area of sky over which absorption takes place, and
- (c) the height of the absorbing region.

Much of the disagreement may be explained in terms of the following experimental factors:

- (i) use of photometers and riometers with widely different fields of view

\* Antarctic Division, Department of External Affairs, Melbourne, and Physics Department, University of New South Wales, Kensington, N.S.W.; present address: Department of Space Science, Rice University, Houston, Texas.

† Antarctic Division, Department of External Affairs, Melbourne; present address: Mawson Institute for Antarctic Research, University of Adelaide.

- (ii) failure to allow for the side lobes of riometer aerial patterns. This could be particularly important if simple three-element Yagis have been used (see Ansari 1963 for a full discussion)
- (iii) lack of detailed consideration of the auroral geometry present throughout the absorption event
- (iv) failure to allow for "van Rhijn" effects on auroral intensity when wide fields of view have been used. Similarly the obliqueness of the signal received by the riometer could be important. Errors of the order of 50% could result from these effects if the absorption occurred near the edge of the field of view of wide-field instruments

The above criticisms will be referred to as criticisms (i), (ii), (iii), and (iv) in the following discussion.

*(a) Simultaneity of Absorption and Aurora*

Holt and Omholt (1962), using a photometer and a 27.6 Mc/s riometer, found "reasonably good correlation" between auroral absorption and intensity. They found a time delay between outbursts of aurora and increases in absorption ranging from less than 1 to up to 10 min. Such time lags could be explained by criticism (i), as the fields of view of photometer and riometer were quoted as being 5° and 30° respectively. A three-element Yagi aerial was used, so criticism (ii) would also be important. All-sky photographs for the events discussed were not published. Holt and Omholt also state that their results were "consistent with, although not proof for, the view that X-rays generated by bremsstrahlung are responsible for *D*-region ionization"; the present authors feel that this conclusion, together with the discussion concerning characteristic electron lifetimes and speculations on electron energy spectra, is not warranted by the data.

Holt, Landmark, and Lied (1961) used a network of five closely spaced riometer stations and studied an auroral absorption event in conjunction with all-sky photographs. They found "good agreement between absorption and auroral luminosity" but indicated that the correspondence was not one-to-one. Three-element Yagi antennas were used, so cases of lack of correspondence could be explained by criticism (ii).

Ansari (1963), using a narrow-beam riometer (12°) antenna switched from 12° N. to 12° S. of the zenith, made a study of auroral intensity and absorption by comparing the absorption data with two  $\lambda 5577$  photometers (6° field of view) directed 12° N. and 12° S. of the zenith. Ansari allowed for side-lobe contamination of absorption measurements and presents a number of plots that show two types of relationships between intensity and absorption. Prior to and during auroral breakup the absorption and intensity correlated intimately, with no time lag between peaks. The absorption in this phase was found to be limited to the luminous regions of the sky. After the breakup the correlation was not good and a 10- to 100-fold increase in the ratio of absorption to intensity was observed. During this latter phase the absorption events were more slowly varying and widespread in character.

(Similar results were obtained by the present authors from Antarctica during 1963; see Section III(i).)

Gustafsson (1964) studied intensity-absorption relationships with a riometer (three-element Yagi) and a photometer ( $5^\circ$  field of view). The time lag observed could thus be explained by criticisms (i), (ii), and (iii). However, Gustafsson used the observed time lag to infer an effective ion production rate greater than that predicted theoretically for X-rays (Omholt 1960) and concluded that the main part of the absorption was due directly to ionizing particles. The present authors feel that little reliance can be put on Gustafsson's conclusions.

#### (b) *The Absorbing Area*

Chapman and Little (1957) suggested that absorption should be more widespread than visual aurora, being due mainly to bremsstrahlung X-rays produced by primary auroral electrons. This proposal was based on early estimates of 100 keV X-ray fluxes, now regarded as being many orders of magnitude too high for auroral electrons.

Ansari's (1963) results did not support the Chapman-Little theory, at least not in the pre-breakup and breakup period. Ansari calculated that, for electrons of 10 keV energy, the absorption as a result of *D*-region ionization by bremsstrahlung X-rays was only 2.5% of the absorption resulting from direct ionization by the incoming electrons.

Hultqvist (1964) presented calculations similar to Ansari's, but for electron energy spectra as observed from rockets (McIlwain 1960; Mann, Bloom, and West 1963) and found that the absorption produced by bremsstrahlung X-rays amounted to 6% of the absorption due to direct ionization. Brown (1964) obtained similar results.

#### (c) *Height of the Absorbing Region*

Early investigations with ionosondes of the absorption associated with auroras indicated strong absorption below the reflecting layers. Recently, a number of rocket measurements have given information on the auroral electron energy spectrum and the height of auroral absorption (see Table 1).

If flights into auroras are considered, it is seen that the electron and proton energy spectra measured are rather variable. Reasonable limits for the primary electron energy spectrum may be set at  $\exp(-\epsilon/5)$  to  $\exp(-\epsilon/25)$  in the energy range  $3 < \epsilon < 30$  keV. Observations of harder spectra have not been accompanied by auroral observations (note, however, that Ansari (1963) invokes a harder electron energy spectrum for post-breakup precipitation). Very little information is available on the proton energy spectrum but, tentatively, we might assume fluxes of  $10^5$  protons  $\text{cm}^{-2} \text{sec}^{-1} \text{sr}^{-1}$  for energies greater than 100 keV and  $5 \times 10^2$  protons  $\text{cm}^{-2} \text{sec}^{-1} \text{sr}^{-1}$  for energies greater than 500 keV as being reasonable, but not necessarily average (see Table 1). There seems to be little doubt that both electron and proton energy spectra could be subject to considerable variation. This implies that, for a given flux, aurorally associated absorption will also undergo variations in both height and magnitude.

TABLE I  
ROCKET MEASUREMENTS OF AURORAL PARTICLES

Reference	Electrons	Protons	Comments
Meredith <i>et al.</i> (1958)	Flux at 35 keV $\frac{1}{10}$ that at 8 keV. Corresponds to a spectrum varying as $\exp(-\epsilon/8.3)$		Flight made into rayed aurora
McIlwain (1960)	(i) Fairly flat spectrum from 4–10 keV decreasing suddenly above 10 keV. Peak flux $5 \times 10^{10} \text{ cm}^{-2} \text{ sec}^{-1} \text{ sr}^{-1}$ (ii) Energy spectrum varying as $\exp(-\epsilon/5)$ in 3–30 keV range. Flux above 30 keV too small for interpretation	For $E > 100 \text{ keV}$ , flux $< 4 \times 10^3 \text{ cm}^{-2} \text{ sec}^{-1} \text{ sr}^{-1}$  Flux $2.5 \times 10^6 \times \exp(-E/30)$ for $80 < E < 250 \text{ keV}$ . Total flux $\sim 1.6 \times 10^7 \text{ cm}^{-2} \text{ sec}^{-1} \text{ sr}^{-1}$	Estimated that 75% of auroral intensity produced by 6 keV electrons in bright aurora. No H $\beta$ detected on ground  Flight made into auroral glow. 60 R H $\beta$ detected from ground. Hultqvist (1964) calculated peak absorption at 95 km
Davis, Berg, and Meredith (1960)	(i) Energy flux of 0.5–2.5 $\text{erg cm}^{-2} \text{ sec}^{-1} \text{ sr}^{-1}$ in range 8–100 keV with spectrum varying as $\epsilon^{-1}$ . For energies $< 1 \text{ keV}$ , flux $< 10^9 \text{ erg cm}^{-2} \text{ sec}^{-1} \text{ sr}^{-1}$ (ii) Energy flux 0.01–0.06 $\text{erg cm}^{-2} \text{ sec}^{-1} \text{ sr}^{-1}$	Flux of order $10^6 \text{ cm}^{-2} \text{ sec}^{-1} \text{ sr}^{-1}$ for energies $> 100 \text{ keV}$	Flight made into fading rayed structure
McDiarmid, Rose, and Budzinski (1961)	Spectrum varying as $\exp(-\epsilon/22)$ for energies $> 30 \text{ keV}$ ; flux $2 \times 10^6 \text{ cm}^{-2} \text{ sec}^{-1} \text{ sr}^{-1}$	Flux of order $5 \times 10^3 \text{ cm}^{-2} \text{ sec}^{-1} \text{ sr}^{-1}$ For $E > 500 \text{ keV}$ , flux of order $5 \times 10^2 \text{ cm}^{-2} \text{ sec}^{-1} \text{ sr}^{-1}$	Aurora present but not in rocket path Flight made at dawn so not known if any aurora associated with absorption (2–4 dB). Riometer shows slowly varying post-breakup type event. Absorption at 65–90 km, max. at 70–75 km (Heikkila and Pendstone 1961)
Mann, Bloom, and West (1963)	Spectrum varying as $\exp(-\epsilon/25)$ , or as $\exp(-\epsilon/41)$ during magnetic storms		Satellite observation. Harder spectrum observed mainly during magnetic storm. No relation to aurora discussed. Hultqvist (1964) calculated peak absorption at 78 km
McDiarmid and Budzinski (1964)	Spectrum varying as $\exp(-\epsilon/12)$ but can change greatly with time, especially at low energies	For $E > 60 \text{ keV}$ , flux is small compared with electron flux above 40 keV	Flight during small (1 dB) auroral absorption event. Presence of aurora not discussed

Multifrequency riometer measurements (Ziauddin 1961) and time constants derived from absorption measurements (Gustafsson 1964) have indicated low *D*-region altitudes for auroral absorption. Uncertainties involved in upper atmosphere parameters used in the calculations could cause considerable error in height calculations from such measurements.

On the other hand, studies of auroral absorption during twilight (Brown and Barcus 1963; Hultqvist 1963*a*, 1963*b*) and the day/night ratio of auroral absorption (Brown 1964*b*) have led to the conclusion that absorption takes place above 90 km, or, alternatively, that the ratio ( $\lambda$ ) of negative ion to free electron density is much less than hitherto believed (Hultqvist 1963*a*, 1963*b*).

Campbell and Leinbach (1961) calculated the absorption occurring in the height interval of visual aurora from the measured intensity profile and the ratio of ionization and excitation cross sections for electrons. They concluded that all auroral absorption could conceivably take place in the height interval of the visual form.

It is not clear from Ansari's (1963) calculations at what height the absorption is supposed to take place. He refers to absorption as being due to *D*-region ionization by auroral electrons with energies less than 20 keV; such electrons, however, would penetrate only to 98 km (Rees 1964).

Hultqvist (1964) used measured (rocket) electron energy spectra to calculate the height of auroral absorption (see Table 1). However, after considering experimental values of the day/night ratio of auroral absorption and assuming an equal contribution from the steep and flat energy spectra considered, he concluded that the main part of the absorption occurs below 90 km. Uncertainties in atmospheric parameters used and the assumptions on energy spectra give little confidence in this result.

Brown (1964*a*) concluded that an energy spectrum varying as  $\exp(-\epsilon/\beta)$  (with  $\beta < 10$  keV) was consistent with experimental data on total energy input, with the magnitude and day/night ratio of auroral absorption, and with X-ray observations at balloon altitudes. (Exponential spectra with greater values of  $\beta$ , or power-law spectra, gave absorption values and day/night ratios exceeding experimental values.) Brown calculated the absorption peaks for  $\beta = 5$  and 10 keV to be at 93 and 85 km respectively.

Parthasarathy and Berkey (1965*a*) used multistation and multifrequency riometer data to study auroral zone sudden onset absorption events. They concluded that the absorption was "somewhat" localized in space and that the luminous features of the display were "to be interpreted as concomitant effects rather than causative factors" in the absorption. However, their Figure 11 shows a close dependence of absorption on auroral coverage of the antenna patterns. The low correlation between absorption events at different stations is only to be expected from the irregular geometry of the aurora at breakup. Similarly, little correlation is to be expected with magnetic data, as electric currents associated with auroras outside the field of view of the riometers will still affect the magnetograms. Criticism (ii) is particularly applicable in this case.

Recently, Parthasarathy and Berkey (1965*b*) used multistation and multi-frequency riometer data to investigate the electron density content in the *D* region during certain types of absorption events, namely, those characterized by a smooth variability and widespread geographic extent. (Such events may include the SVIA type events discussed in the present paper.) The general features of the derived profiles were found compatible with ionization due to high energy electrons and associated bremsstrahlung X-rays.

Simultaneous balloon observations of bremsstrahlung X-rays and auroral intensity (Barcus 1965) showed a "rather loose correlation" (in the sense of a detailed space-time association). Barcus suggests that essentially different, though not infrequently coupled, mechanisms are responsible for the high and low energy portions of the precipitated electron energy spectrum. Detailed analysis of an absorption event at auroral breakup indicated that the absorption could be accounted for by the same flux of low energy electrons responsible for the simultaneous intensity enhancement. This suggests that the height of the absorbing region was  $\sim 100$  km.

## II. EXPERIMENTAL DETAILS

Observations aimed at resolving some of the uncertainties discussed above were carried out at Mawson, Antarctica (eccentric dipole geomagnetic co-latitude  $19^\circ$ ) during the winter of 1963. The following equipment was used:

- (i) A riometer (27.6 Mc/s) with a field of view of  $27^\circ$  and negligible side-lobe contamination of the aerial pattern. (Side lobes at  $40^\circ$  were 13 dB down on the main zenithal lobe.) This was achieved by using a 4 by 2 array with an element spacing of  $\frac{1}{2}\lambda$  and height above the earth matt of  $\frac{1}{4}\lambda$ .
- (ii) A zenith photometer ( $\lambda 5577$ ) with a similar field of view ( $23^\circ$ ) and calibrated absolutely; the recording range was logarithmic from 1 to 500 kR.

Both riometer and photometer had small time constants and high recording speeds for good time resolution. Riometer fall time was  $< 0.5$  sec, rise time 1 mm/sec (chart width 40 mm); photometer time constant  $< 0.5$  sec; recording speed 5 mm/min.

- (iii) A photometer to monitor  $H\beta$  intensity, sensitivity 1 R.
- (iv) A riometer at 77 Mc/s with a field of view (zenithal) of  $13^\circ$  during the latter part of the investigation.
- (v) All-sky cameras, magnetographs, and an ionosonde.

Visual auroral observations were made at 10 min intervals, and more frequently during active aurora, so that a continual record of auroral type was obtained.

All instruments were controlled from the same crystal chronometer and the time accuracy on all records was better than 5 sec.

Some 80 nights of observations were obtained from cloudless skies and without equipment malfunction. There was usually at least one auroral type absorption event during each night.

## III. OBSERVATIONS AND RESULTS

*(a) Types of Absorption Events*

The 27.6 Mc/s riometer records were scaled every 15 min of sidereal time throughout the year and monthly average curves of diurnal absorption (converted to U.T.) are shown in Figure 1. There are two well-defined maxima, one about local midday and the other 1–2 hr after local midnight. The night-time maximum is due to absorption events associated with visual aurora and includes both sudden ionospheric absorption events (SIA) typical of the auroral breakup, and slowly varying ionospheric absorption events (SVIA) typical of the post-breakup phase. The day-time maximum is due to a small number of SIA-type events but mostly to SVIA type.

Typical riometer records are shown in Figure 2 (Plates 1 and 2) along with all-sky photographs. Figure 2(a) (Plate 1) shows a slowly varying day-time absorption event typical of those giving rise to the day-time maximum of the diurnal curves. Figure 2(b) (Plate 1) shows a weak absorption event associated with quiet arcs and bands in the pre-breakup phase. Figure 2(c) (Plate 1) shows a typical sudden onset event associated with an auroral breakup. Also shown in Figure 2(c) is the  $f_{\min}$  plot for the event. Note that total blackout lasts only for the duration of the SIA event. Absorption frequently reached 10 dB in  $\sim 20$  sec. Sometimes the level recovered to the quiet day level in times of the order of 5 min (as in Fig. 2(c)), but often recovery took 30–60 min and during this time absorption fluctuated much more slowly. This type of behaviour is shown in Figure 2(d) (Plate 2). Figure 2(e) (Plate 2) shows the low  $\lambda 5577$  intensity recorded on the zenith photometer during an SVIA event. The  $f_{\min}$  plot shows blackout for about 1 hr (the duration of the SVIA event). During this slowly varying post-breakup phase a diffuse glow (sometimes subvisual) covered the sky, and the ratio of absorption to intensity sometimes increased by a factor of the order of 100. Similar results from Alaska have been reported by Ansari (1963). Figure 2(f) (Plate 2) shows similar events to those shown in Figures 2(b)–2(d), all occurring within a few hours.

*(b) Day/Night Absorption Ratio*

The average day/night ratio for all absorption events (excluding possible PCA events) was determined for each month. Monthly averages ranged from 0.8–1.6 with an overall yearly average and standard deviation of  $1.25 \pm 0.25$ . A total of 163 day-time events and 146 night-time events were considered in this analysis. The day/night ratio has been used to estimate the height of the absorbing layer (Brown and Barcus 1963; Hultqvist 1963a, 1963b; Brown 1964b). Both the first and last authors distinguished between slowly varying and sudden onset type events when determining the day/night ratio, and in both cases they found a ratio of essentially unity. In the present investigation most day-time events were slowly varying in character, though typically had sudden onsets, whereas most night-time events showing strong absorption were SIA, so it was not possible to obtain separate day/night ratios for the two types of events.

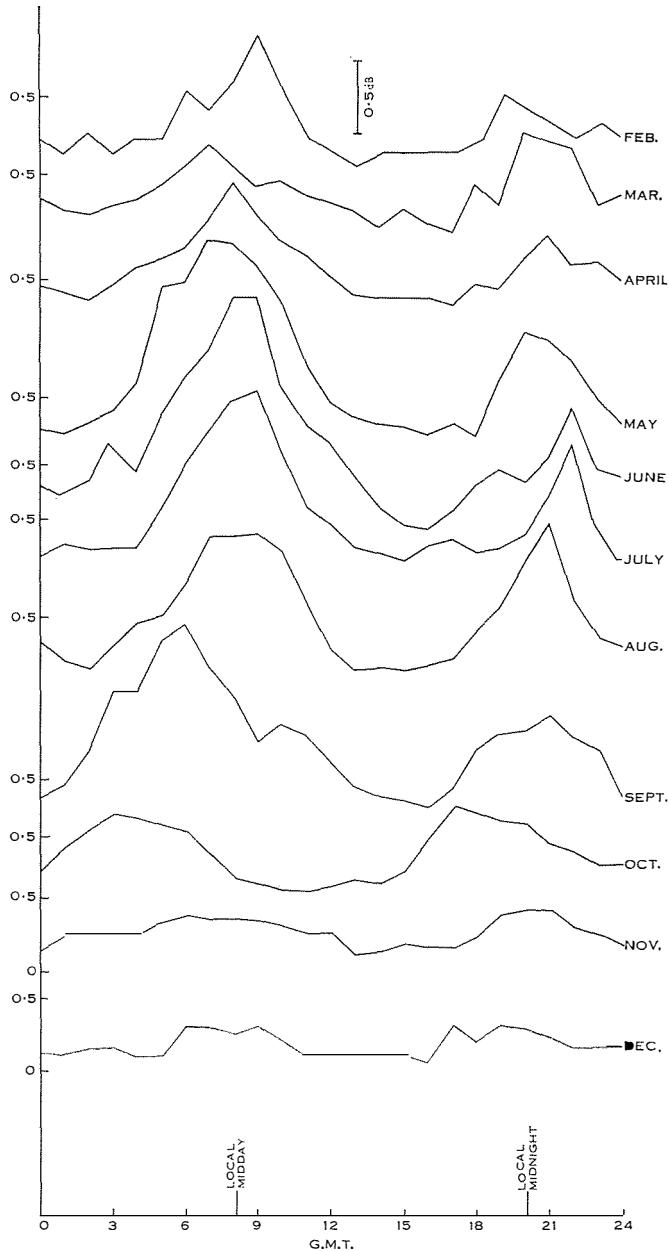


Fig. 1.—Monthly average curves of diurnal riometer absorption at 27.6 Mc/s for Mawson, 1963.

Brown (1964) considers electron energy spectra varying as  $\exp(-\epsilon/\beta)$  and calculates day/night ratios of 1.05, 1.25, and 1.6 for  $\beta = 5, 10,$  and  $20$  keV respectively, and corresponding absorption peaks at 93, 85, and 80 km. The value of 1.25 obtained by the present authors suggests a height of 85 km, though this

AURORAL ABSORPTION OF COSMIC RADIO NOISE

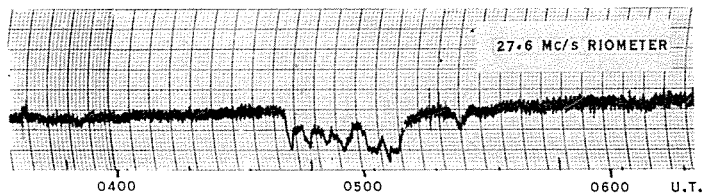


Fig. 2(a).—27.6 Mc/s riometer record for September 22, 1963, showing typical day-time absorption event.

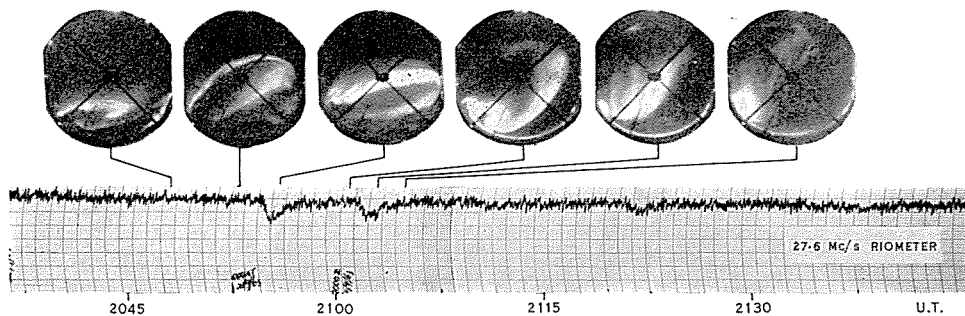


Fig. 2(b).—27.6 Mc/s riometer record and all-sky camera photographs for September 20, 1963, showing weak absorption due to quiet auroral bands (qHB2a).

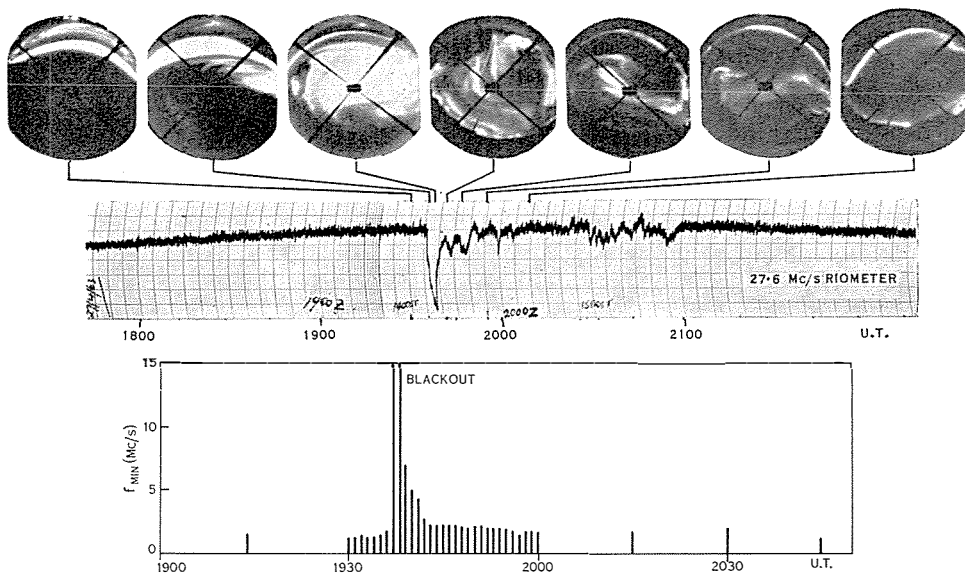


Fig. 2(c).—27.6 Mc/s riometer record and all-sky camera photographs for April 27, 1963, showing a typical SIA event. The  $f_{min}$  plot for the event is also shown.

## AURORAL ABSORPTION OF COSMIC RADIO NOISE

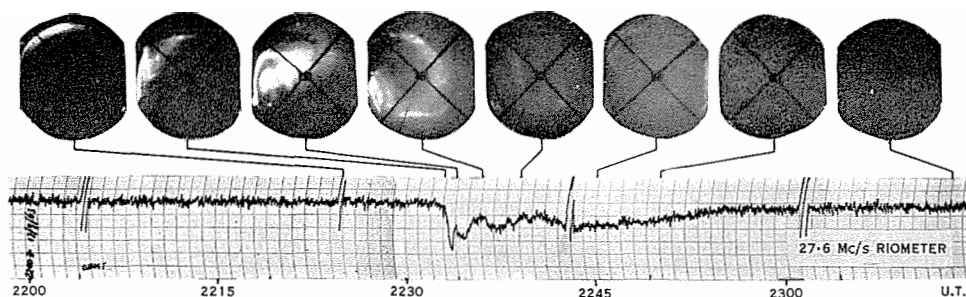


Fig. 2(d).—27.6 Mc/s riometer record and all-sky camera photographs for September 17, 1963, showing a typical SVIA event. Note the weak diffuse luminosity associated with the prolonged absorption.

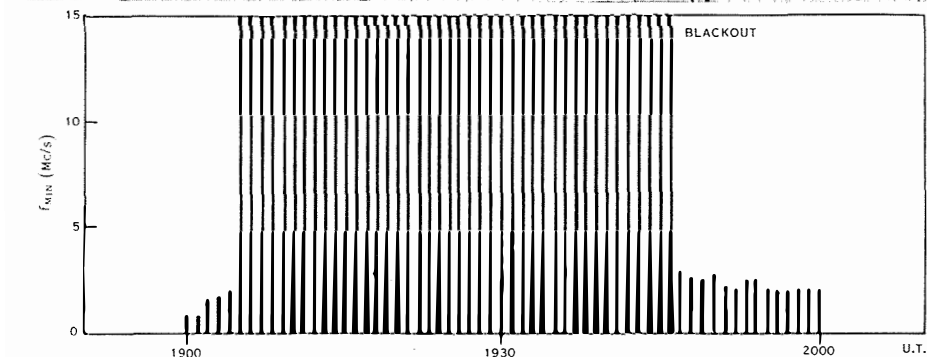
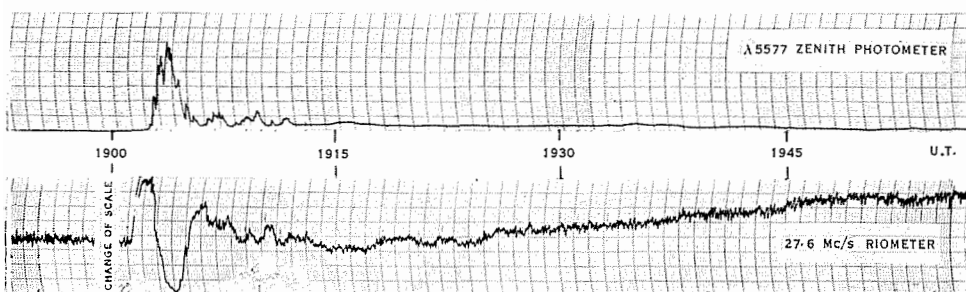


Fig. 2(e).—27.6 Mc/s riometer record and  $\lambda 5577$  zenith photometer record for September 16, 1963, showing a SIA event developing into a SVIA event. The  $f_{\min}$  plot for the event is also shown.

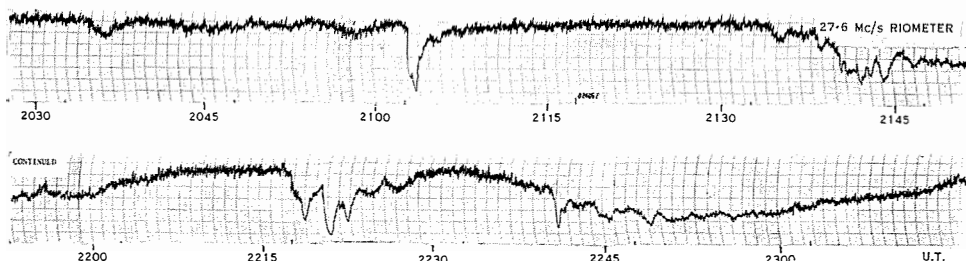


Fig. 2(f).—27.6 Mc/s riometer record for September 7, 1963, showing the three types of night-time auroral absorption events occurring within a few hours.

AURORAL ABSORPTION OF COSMIC RADIO NOISE

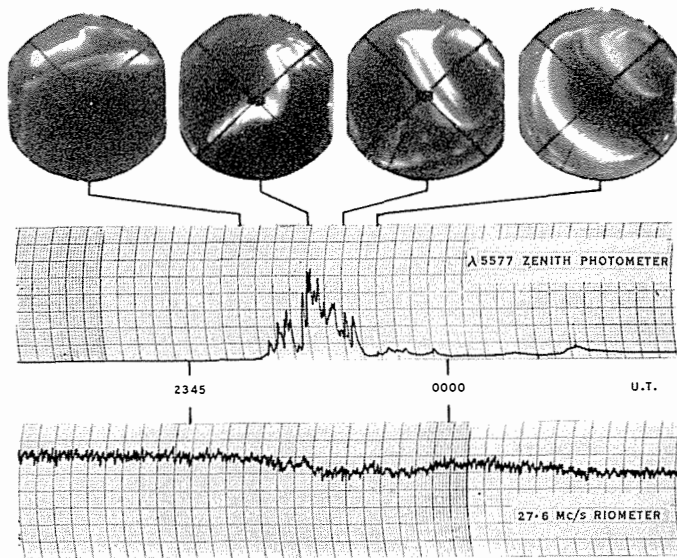


Fig. 3.—27.6 Mc/s riometer record,  $\lambda 5577$  zenith photometer record, and all-sky camera photographs for September 13, 1963. An intense thin auroral band in the zenith gives high luminosity but little absorption.

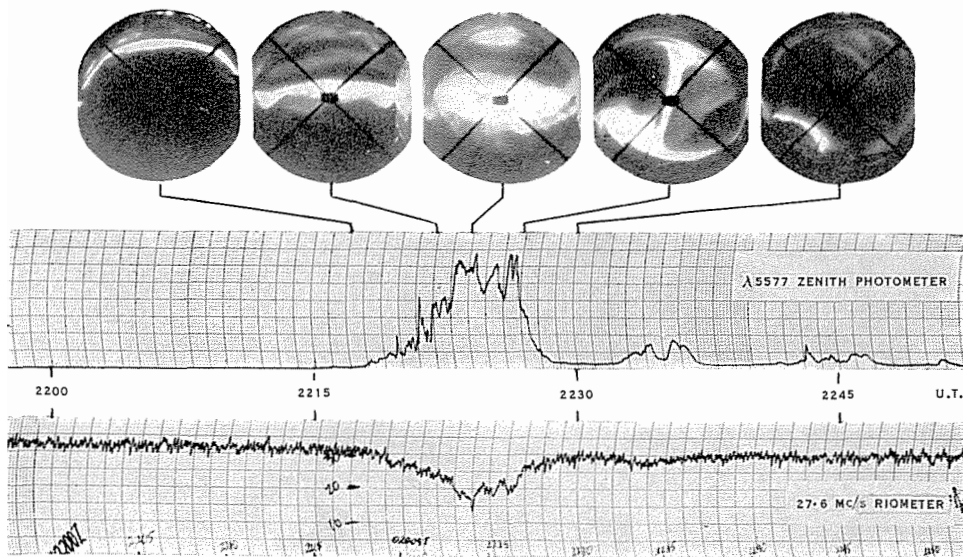


Fig. 4.—27.6 Mc/s riometer record,  $\lambda 5577$  zenith photometer record, and all-sky camera photographs for September 13, 1963, showing how intensity peaks may precede absorption peaks.



is rather uncertain because of the different character of the day and night events. It may be that the electron energy spectra responsible for day and night absorption are quite different. One might in fact expect different energy spectra from the different orientation of the day and night hemispheres with respect to the distorted magnetosphere. If the ratio for both types of events is in fact unity (Brown and Barcus 1963; Brown 1964b), then the ratio of 1.25 obtained suggests a harder electron energy spectrum as being responsible for the day-time events. Alternatively, average day-time electron fluxes may be greater than those at night.

### (c) *Two-frequency Measurements*

A 77 Mc/s riometer was in operation during the last 6 weeks of the auroral season. During this period there were 24 SIA events giving absorption greater than 0.5 dB at 77 Mc/s.

The average ratio of absorption at 27.6 and 77 Mc/s was determined for these events as  $7.9 \pm 2.0$ . The theoretical ratio for  $\omega \gg \nu$  is 8.1 (see Appendix I). Thus all absorption takes place in the region where  $\omega \gg \nu$ . On current estimates of the height dependence of  $\nu$  (Hultqvist 1964) this places the main absorbing region at a height  $> 80$  km.

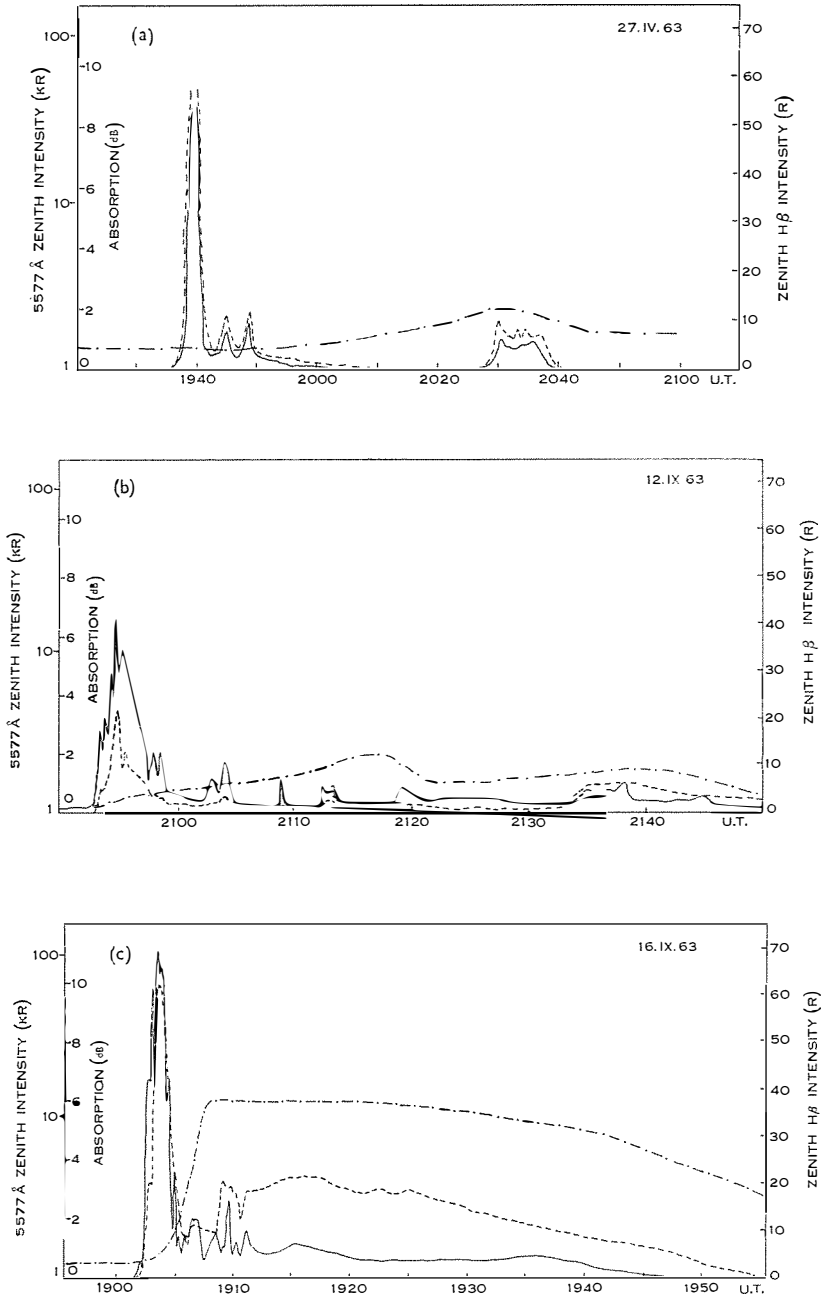
The standard error in the observed ratio is probably due to auroral geometry effects, variable electron energy spectra, and deviations from the "thin" absorbing region of the theory (so that appreciable changes in  $\nu$  and  $N$  could occur over its thickness).

### (d) *The Absorbing Area*

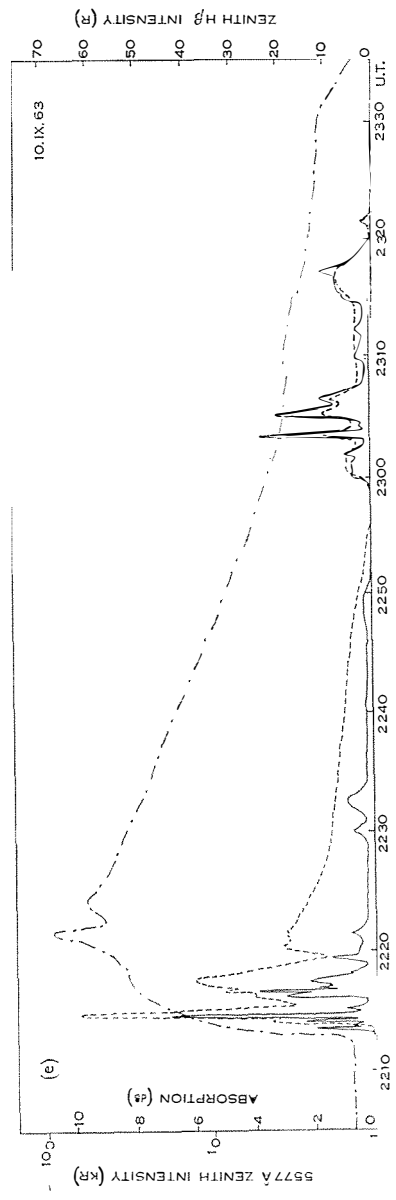
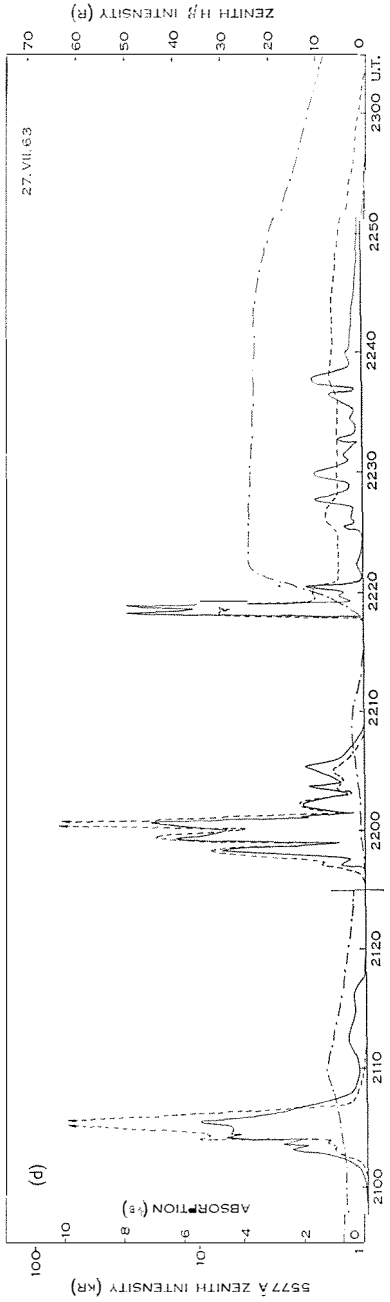
Examination of auroral absorption, zenith photometer, and all-sky camera records for over 100 auroral absorption events of the pre-breakup and breakup phases showed no cases of absorption being recorded without aurora in the field of view of the riometer antenna. It thus seems certain that, in the breakup and pre-breakup phases of auroral activity, measurable absorption at 27.6 Mc/s takes place only in the region of sky of the aurora. Absorption resulting from bremsstrahlung X-rays from auroral primaries is unimportant for these events.

A number of cases of high intensity with little absorption were recorded. In all cases these could be explained in terms of the auroral geometry at the time; they were due to intense narrow auroral bands covering only a fraction of the field of view of the riometer and zenith photometer. (Complete absorption in a band covering say 10% of the field of view would only give rise to 0.45 dB absorption.) A typical example of such an event is shown in Figure 3 (Plate 3).

As mentioned before, strong absorption associated with low values of intensity was observed in post-breakup SVIA type events. Ansari (1963) found that this strong absorption occurred over the whole sky during such events. The aurora associated with these events was typically diffuse and patchy over the whole sky and of brightness index 1. (Sometimes discrete active forms near the southern horizon were also present.) Bremsstrahlung X-rays could possibly contribute to the absorption during this phase.



Figs 5(a) to 5(e).—27·6 Mc/s riometer absorption,  $\lambda 5577$  zenith intensity, and  $H\beta$  zenith intensity for a number of SIA and SVIA events. The  $H\beta$  intensity remains essentially unchanged during and after SIA events, whereas it shows a marked increase during SVIA events.  $\lambda 5577$  intensity is intimately correlated with absorption during SIA events, but shows little relationship during SVIA events. (Figs 5(d) and 5(e) are on the opposite page.)



Figs 5(d) and 5(e)

*(e) Simultaneity of Intensity and Absorption*

A typical auroral breakup event at Mawson begins when quiet homogeneous arcs and bands near the northern horizon become active and increase in intensity—the active bands move rapidly towards the zenith and spread across greater areas of the sky. A sequence of all-sky photographs illustrating this behaviour is shown in Figure 2(c) (Plate 1).

For all cases of widespread active aurora moving rapidly to the zenith, no time lag was observed between the intensity peak and the absorption peak. With the high chart speeds and low recording time constants used it was possible to estimate the simultaneity at better than  $\pm 5$  sec. Observed cases of time lag were due to thin bright bands moving to the zenith before spreading, and this could lead to intensity peaks preceding absorption peaks. This sort of behaviour was unusual; an example is shown in Figure 4 (Plate 3).

The simultaneity of occurrence of intensity and absorption peaks and the typical detailed correlation between sustained fluctuations in intensity and absorption can be seen in Figures 5(a) to 5(e). This behaviour is predicted by the theory outlined in Appendix II. It is only in cases of stepwise intensity increases that a time lag would be expected. These are rare but in the few cases observed, when the intensity remained high for times of the order of 1 min, the time lag was  $< 5$  sec.

The theory discussed in Appendix II shows that if there is a time lag between intensity and absorption, it will be greater for events with low maximum absorption. Riometer and photometer records were compared for events where the maximum absorption reached was  $< 1$  dB, and again no time lag was ever observed. An example of this is seen in Figure 6, where the auroral intensity shows a sudden increase. The absorption closely follows the intensity, and there is no time lag between peaks.

Theoretical values for the time lag for step-function type increases in intensity were calculated as follows. The absorption at 27.6 Mc/s is given by

$$dA/dh = 4.59 \times 10^4 N\nu(3.34 \times 10^{16} + \nu^2)^{-1} \quad \text{dB/km,}$$

where  $N$  is the electron density and  $\nu$  the electron collision frequency. In the height region above 70 km, this may be approximated by

$$dA/dh = 1.37 \times 10^{-12} N\nu.$$

Using Brown's (1964*a*) absorption curves (adjusted to give a total of 1 dB absorption) and Hultqvist's (1964) data for  $\nu$ , the electron density  $N$  was calculated throughout the absorbing layer. The time lag  $t_{90}$  defined in Appendix II can then be calculated throughout the absorbing layer for the different electron energy spectra considered by Brown (1964*a*), and the resultant curve of  $t_{90}$  as a function of height is shown in Figure 7.  $t_{90}$  thus varies considerably throughout the absorbing layer, and with the assumed energy spectrum. The effective time lag for the complete absorbing layer  $\tau_{90}$  is given by the solution of

$$\int_0^\infty \frac{dA}{dh}(h, t) dh = 0.9,$$

where  $t$  is the time measured from the step-function increase in auroral intensity.

$\tau_{90}$  and also  $\tau_{70}$  were calculated by numerical methods for the absorption curves of Figure 7, and the results were:

$$\begin{aligned} \tau_{90} (\beta = 5) &= 7.0 & \tau_{70} (\beta = 5) &= 3.0 \\ \tau_{90} (\beta = 20) &= 60.0 & \tau_{70} (\beta = 20) &= 23.0 \end{aligned}$$

From Appendix II, if the final equilibrium value of absorption were  $A_0$ , then the time for the absorption to reach 90% (70%) of its original value would be  $\tau_{90}/A_0$  ( $\tau_{70}/A_0$ ).

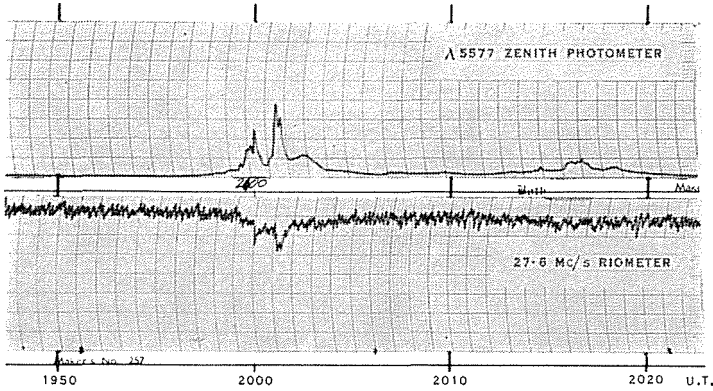


Fig. 6.—27.6 Mc/s riometer and  $\lambda 5577$  zenith intensity for a sudden onset event with maximum absorption  $\sim 1$  dB. There is no time lag between peaks and the riometer follows auroral intensity spikes of total duration  $\sim 10$  sec.

The experimental result that any time lag between intensity and absorption is  $< 5$  sec for SIA events, for peak absorption ranging from 1 to  $\sim 12$  dB, is consistent with the following interpretation.

- (i) In all cases examined, the rise time of auroral luminosity was  $> 20$  sec (see figures for examples). Thus theoretical  $\tau_{90}$  values would be less than those calculated above for step-function type intensity increases.
- (ii) In the cases of high maximum absorption values, the absorption could have been due to electron energy spectra with  $\beta$  values in the range 5–20 keV.
- (iii) In cases of low maximum absorption, the absence of any time lag suggests that the absorption was due to an electron energy spectrum with low  $\beta$  values ( $\sim 5$  keV), but in view of (i) above this is rather uncertain.

#### (f) Riometer Recovery Rates

Events were selected for which the riometer showed fast recovery times, and then the zenith photometer records were examined to see if the riometer recovery rate was limited by the rate of decay of auroral intensity, or was in fact a measure of the “relaxation time” of the ionosphere at the height of the absorbing layer. In all cases examined (30 events showing fast riometer recovery), the riometer

recovery rate was either limited by the auroral intensity decay rate (see Fig. 8) or by the instrumental rise time.

Those events in which the recovery rate was limited by the instrumental rise time were considered as follows. The time taken for the absorption to fall to one-tenth of its initial value was calculated, assuming that the recovery rate would be limited by the instrumental rise time over the whole recovery time. This assumption is justified, as events were observed in which the maximum absorption was  $\sim 1$  dB and yet the recovery rate of the riometer was still limited by the instrumental

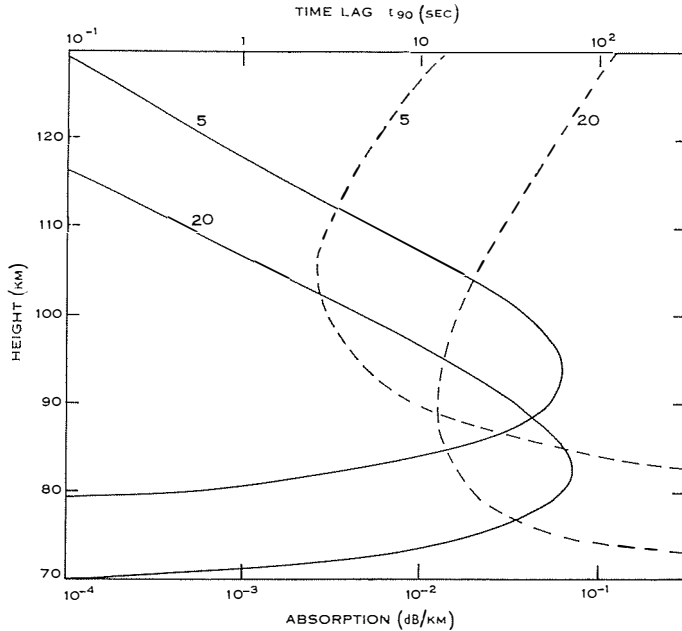


Fig. 7.—Absorption at 27.6 Mc/s for electron spectra varying as  $\exp(-\epsilon/\beta)$  with  $\beta = 5$  and 20 keV (full curves), adjusted to give a total absorption of 1 dB (after Brown 1964*a*), and riometer relaxation times (dashed curves) calculated through the absorption profiles.

rise time. These values were then multiplied by the initial absorption  $A_0$  to give the time corresponding to an initial 1 dB absorption ( $t'_{90}$ ). It was thus concluded that

$$\tau'_{90} < 31 \text{ sec.}$$

Actual  $\tau'_{90}$  values could be much less than 31 sec, as all these events were limited by the instrumental rise time.

The theory of Appendix II shows that, at a given height and for a step-function decrease in auroral intensity,

$$t'_{90} = 9/\alpha N.$$

As in the previous section, the effective time  $\tau'_{90}$  for the complete absorbing layer

is given by the solution of

$$\int_0^{\infty} \frac{dA}{dh}(h, t) dh = 0.1.$$

Numerical calculations from the curves of Figure 7 give

$$\begin{aligned} \tau'_{90}(\beta = 5) &= 35.0 \text{ sec,} \\ \tau'_{90}(\beta = 20) &\sim 160 \text{ sec.} \end{aligned}$$

The experimental result that  $\tau'_{90}$  is less than 31 sec for the 30 fast recovery events considered suggests that the electron energy spectra responsible for these events were characterized by values of  $\beta \sim 5$  keV.

All other SIA events showed recovery times longer than the fall time of intensity, and longer than the instrumental rise time. Measured  $\tau'_{90}$  values varied from 31 to 258 sec, which are consistent with absorption caused by electron energy spectra with  $\beta$  values between 5 and  $\sim 25$  keV.

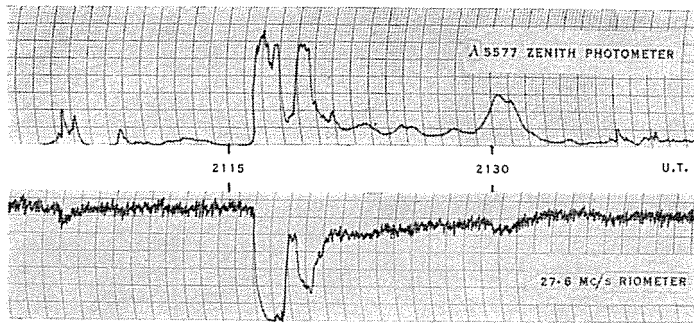


Fig. 8.—An example of rapid riometer recovery after an SIA event, where the recovery rate is not limited by the rate of decrease of auroral intensity, but is limited by the instrumental rise time.

Thus the measurements discussed in Sections (e) and (f) above are all consistent with electron energy spectra varying as  $\exp(-\epsilon/\beta)$ , with  $\beta$  taking values between slightly less than 5 and  $\sim 25$  keV. Such energy spectra give heights of maximum absorption ranging between 80 and 95 km (Brown 1964a).

#### (g) *The Intensity/Absorption Ratio*

The maximum intensity reached during all auroral absorption events of magnitude greater than 0.5 dB in the breakup phases was plotted against the maximum absorption. Spike-type intensity peaks of duration less than 10 sec were excluded from the analysis because of the possibility that the absorption may not have had time to reach its equilibrium value corresponding to the maximum intensity (see Appendix II). A considerable scatter of points was evident. It is thought that part of the scatter might be due to auroral geometry effects, i.e. variations in the fraction of the field of view covered by aurora. Thus only those

events for which all-sky photographs were available were selected (134 events in all) and allowances for the auroral geometry were made as outlined in Appendix III. Calculations were made assuming that

- (i) all absorption takes place in the region of the aurora, and
- (ii) absorption takes place over the whole field of view.

TABLE 2

CORRELATION COEFFICIENTS BETWEEN  $\lambda 5577$  INTENSITY, ABSORPTION, AND  $K$  INDEX FOR SIA EVENTS

	Intensity	(Intensity) <sup>½</sup>	Absorption		$K$ Index
			Assumption (i)	Assumption (ii)	
Intensity	1.00	—	0.59	0.49	0.18
(Intensity) <sup>½</sup>		1.00	0.69	0.58	0.17
Absorption					
assumption (i)			1.00	—	0.27
assumption (ii)				1.00	0.28
$K$ index					1.00

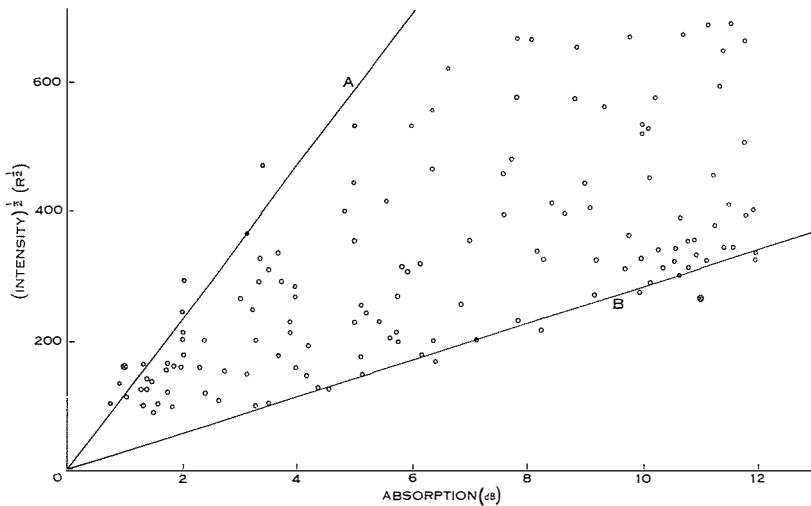


Fig. 9(a).—Square root of maximum intensity plotted against maximum absorption for SIA events. See text for explanation of lines A and B.

The resultant correlation coefficients (all significant at the 1% level) are listed in Table 2. Also, Figure 9(a) shows the square root of maximum intensity plotted against the maximum absorption of the cosmic noise signal, assuming all absorption to take place in the region of the aurora. (Quasi-equilibrium theory predicts that absorption should be proportional to the square root of intensity; see Appendix II.)

The correlation coefficient obtained by using assumption (i) is slightly higher than that obtained by using assumption (ii). Correlation was slightly better between absorption and the square root of auroral intensity, and the correlation coefficient of 0.69 implies that only about half of the variance of the observed absorption can be related directly to changes in intensity.

TABLE 3  
POSSIBLE SETS OF ENERGY SPECTRUM PARAMETERS  $\beta$

Assumed Values (keV)		Extreme Values (keV)	
$\beta_{\min}$	$\beta_{\max}$	$\beta_{\min}$	$\beta_{\max}$
3.0	16.0	—	21.0
4.0	20.0	1.0	23.0
5.0	24.0	2.3	28.0
6.0	27.0	3.3	30.0
7.0	29.0	4.0	—

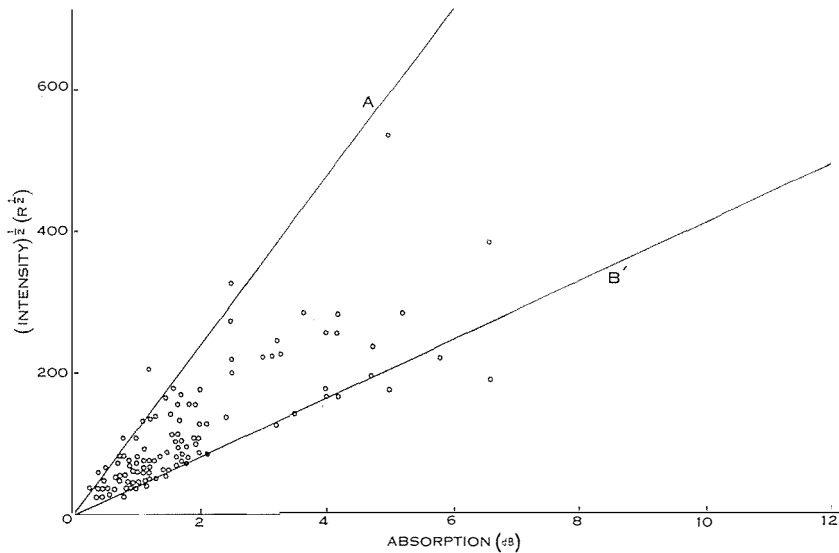


Fig. 9(b).—Square root of intensity plotted against absorption at 1 min intervals during a long SIA event. See text for explanation of lines A and B'.

The only other variable that can account for the scatter of points in Figure 9(a) is the electron energy spectrum. Figure 9(a) can be used to estimate the range in electron energy spectra that is required to explain the observed scatter. Two lines A and B were drawn so that 95% of the points lay above B and 95% of the points below A. It is now assumed that B corresponds to the hardest energy spectrum

normally associated with aurora in the pre-breakup and breakup phases, while line A corresponds to the softest such spectrum.

The softest auroral electron energy spectrum measured by rockets (see Table 1) can be described by the spectrum  $\exp(-\epsilon/\beta)$  with  $\beta = 5$  keV. (Brown (1964a) has also calculated that the absorption caused by such a spectrum for acceptable total energy inputs is of the order of the observed absorption.) Assuming  $\lambda 5577$  intensity/electron production rate to be independent of primary electron energy, taking A as corresponding to  $\beta_{\min} = 5$  keV in Figure 9(a), and using the results of integrating over Brown's (1964a) specific absorption curves, implies that B corresponds to  $\beta_{\max} = 24.0$  keV. Table 3 shows the range of  $\beta_{\min}$  to  $\beta_{\max}$  values required to explain the scatter of points in Figure 9(a) for various assumed softest energy spectra. The  $\beta_{\max}$  values in all cases agree well with experimental measurements by rockets (Table 1), which suggest a value of the order of 25 keV (except for one very hard spectrum with  $\beta \simeq 41$  keV; Mann, Bloom, and West 1963).

Also included in Table 3 are extreme values of  $\beta_{\min}$  and  $\beta_{\max}$  (for the assumed  $\beta_{\min}$ ) as calculated from the extreme points of Figure 9(a). Values of  $\beta < 5$  and  $> 20$  keV were obtained by extrapolation of Brown's (1964a) curves.

From the above discussion and the rocket data of Table 1 it is concluded that the electron energy spectrum responsible for aurora in the breakup phase of an auroral display varies markedly from event to event. An  $\exp(-\epsilon/\beta)$  energy spectrum with  $\beta$  in the range 5–24 keV can describe 90% of the spectra; at times extreme values with  $\beta \sim 2.5$  and 30 keV occur. The least squares straight line fit through the points of Figure 9(a) corresponds to  $\beta = 10$  keV, if line A is assumed to correspond to  $\beta_{\min} = 5$  keV.

The variability of the electron energy spectrum during a single event was examined in a similar way. A number of events that lasted for more than 1 hr were selected and intensity and absorption were scaled every minute. Auroral geometry was allowed for and the resultant plot of square root of intensity against absorption is shown in Figure 9(b) for a 2 hr event. The correlation coefficient in this case is 0.8, and the range of  $\beta$  values required to contain 90% of the points is  $\beta = 5$  to 18 keV. This indicates that the electron energy spectrum also varies markedly during a single event.

#### (h) Correlation with K Index

Table 2 shows low correlation coefficients between auroral intensity and absorption and the  $K$  index. (Although fast-run absolutely calibrated magnetograms were available for all events, the magnetic deflection (in gammas) was not scaled, as normally the maximum magnetic deflection and the maximum intensity and absorption occur at the same time, and more than one breakup event rarely occurred in a 3 hr  $K$ -index period. Thus the  $K$  index, as determined at Mawson, is a good measure of the maximum magnetic deflection.) This poor correlation is not surprising, as the magnetograms are affected by electric currents associated with auroras in all parts of the sky and not just with zenithal forms. The shape of the  $H$ -component record was usually quite different from that of the intensity and absorption records.

However, in cases of breakup events, where the activity was confined to narrow well-defined forms in the zenith, the  $H$ -component records showed intimate correlation with the intensity and absorption records. Figures 10(a) and 10(b) illustrate these points. Brown and Barcus (1963) similarly found that, when auroras were centred over the antenna, there was a good correlation between absorption and perturbation in the horizontal component of the geomagnetic field.

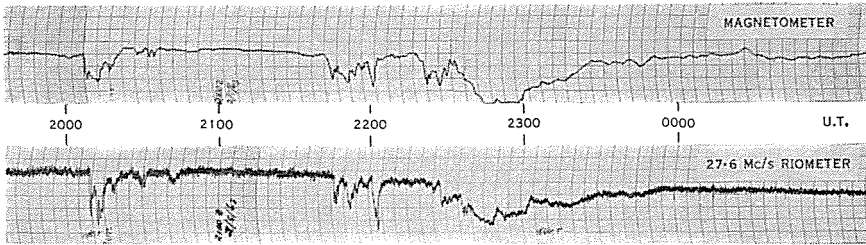


Fig. 10(a).— $H$ -component magnetogram and 27.6 Mc/s riometer record for May 2, 1963, showing excellent correlation between magnetic and absorption fluctuations.

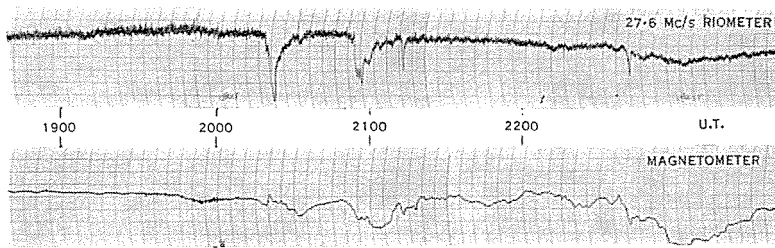


Fig. 10(b).— $H$ -component magnetogram and 27.6 Mc/s riometer record for May 3, 1963, showing little correlation between magnetic and absorption fluctuations.

#### (i) *The Post-breakup Phase*

The previous sections have discussed various aspects of aurorally associated absorption in the pre-breakup and breakup phases of the display. The similarity of intensity and absorption records in these phases is not found in the post-breakup phase when slowly varying type events often occur, lasting some 20 min to 1 hr (see Fig. 2(d), Plate 2). During these SVIA events, absorption fluctuations did not necessarily correspond to intensity fluctuations and the ratio of absorption to intensity increased by a factor up to 100. Faint (sometimes subvisual) diffuse aurora covered the sky during SVIA events. Their slowly varying character and the lack of associated discrete auroral forms suggest that the absorption was more widespread than during SIA events.

These events usually occur late in the night, from 2 to 4 hr after local midnight. If there was more than one breakup event on a given night, the SVIA event usually occurred only after the last breakup event. Sometimes the absorption of the SIA

event had almost returned to zero before the SVIA commenced, while at other times the SVIA event seemed to commence while the SIA event was still in progress (Fig. 2(e), Plate 2). Typically the SVIA absorption was greatest early in the event and recovery was gradual over a 20 min to 1 hr period. Ansari (1963) has reported similar findings from Alaska.

Absorption and intensity were determined every 5 min for all SVIA events for which records were available (260 points in all). The square root of intensity is plotted against absorption in Figure 11 (assuming absorption over the whole field of view). The correlation coefficient between square root of intensity and absorption is 0.31, significant at the 1% level.

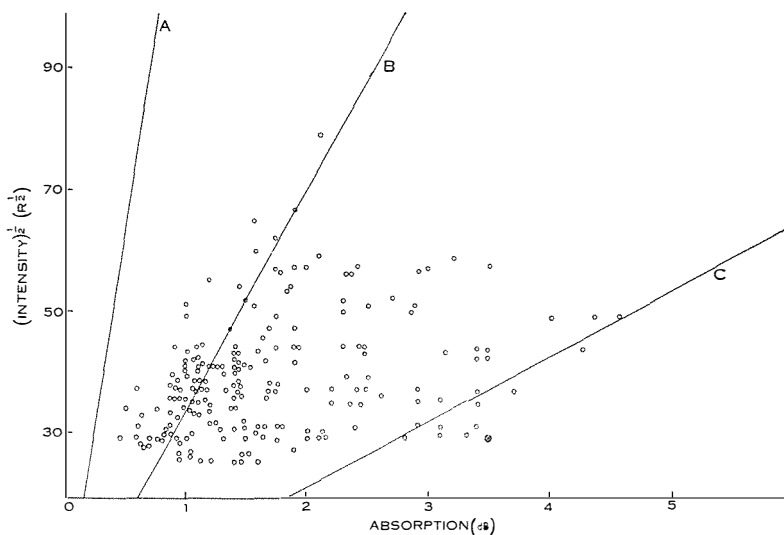


Fig. 11.—Square root of intensity plotted against absorption at 5 min intervals during SVIA events. See text for explanation of lines A, B, and C.

The range of  $\beta$  values required to contain 90% of the points of Figure 11 is 7.5 to approximately 40 keV. Lines A and B are the same lines as drawn in Figure 9(a), while line C is that which has 95% of points above it. The value of 40 keV is obtained by extrapolation of Brown's (1964a) values, but should be accurate to within  $\pm 5$  keV.

#### (j) *The Particles Responsible for SVIA Events*

Ansari (1963) showed that the observed absorption during SVIA events could be explained by a hardening of the electron energy spectrum, and he calculated that an increase in the flux of 30–100 keV electrons to  $10^7$  electrons  $\text{cm}^{-2}\text{sec}^{-1}$  was sufficient to account for most SVIA events.

However, a hardened electron energy spectrum may be only part of the explanation of SVIA events, and the role of protons could be important. Records from the photometer measuring the intensity of  $H\beta$  were examined to investigate

this point further. The  $H\beta$  photometer was being used to study the hydrogen aurora and was normally scanning across the sky; zenith  $H\beta$  measurements were consequently not always available throughout SVIA events. Zenithal  $H\beta$  intensity was recorded for the total duration of 8 SVIA events and 12 SIA events. Some of these events are plotted in Figures 5(a) to 5(e) together with the zenithal  $H\beta$  intensity.

In all cases of SIA that did not develop into SVIA, the  $H\beta$  intensity in the zenith was low and remained essentially unaltered throughout the event. However, in all cases of SIA that developed into SVIA, the  $H\beta$  intensity increased considerably during or just after breakup, and then slowly decreased at about the same rate as the absorption recovered. An example of original records for such an event is shown

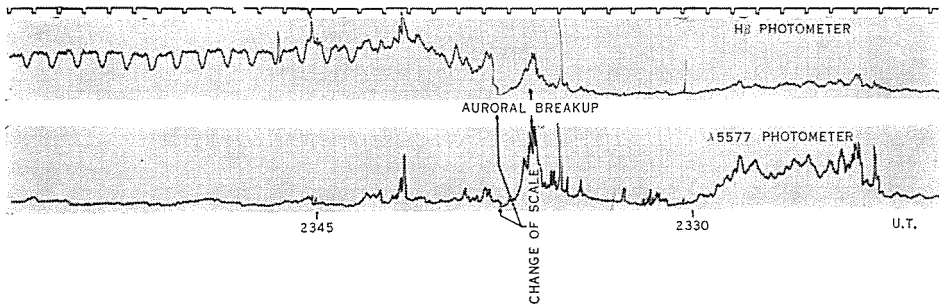


Fig. 12.—Original  $H\beta$  and  $\lambda 5577$  scanning photometer records (photometer fixed in zenith) for June 27, 1963, showing return of hydrogen emission after the auroral breakup. The  $H\beta$  intensity is proportional to the depth of modulation of the photometer trace.

in Figure 12, in which the  $H\beta$  intensity is proportional to the depth of modulation of the photometer trace (the photometer is described in Eather and Jacka 1966). There was no measurable change ( $< \pm 0.6 \text{ \AA}$ ) in the Doppler shift of the peak of the  $H\beta$  line profile during or after the breakup.

Unfortunately, measurements of the Doppler shift of  $H\beta$  give little information on the flux of high energy incident protons. This is because the number of photons produced per incident proton is nearly independent of the initial energy of the protons for energies greater than about 100 keV (see Fig. 7.1, p. 249, of Chamberlain 1961). The  $H\beta$  measurements, then, give an indication only of the incident proton flux. Measured intensities of 10–100 R correspond to proton fluxes of  $10^6$ – $10^7$  protons  $\text{cm}^{-2} \text{sec}^{-1}$ .

Further evidence that SVIA events are due to proton precipitation is provided by the correlation of SVIA with type “r”  $E_s$  ionization. This correlation between  $H\beta$  and  $E_{sr}$  is treated in detail elsewhere (Eather and Jacka 1966), where it is concluded that  $E_{sr}$  is generated by proton precipitation. It is shown that the diurnal variation of zenithal  $H\beta$  exhibits three peaks: the first is associated with the pre-midnight south to north movement of the  $H\beta$  emission zone; the second is associated with SVIA events; the third is associated with the north to south movement of the  $H\beta$  emission zone in the morning hours. The curve of diurnal variation of frequency of occurrence of  $E_{sr}$  also shows three peaks at the same

times. If all occurrences of  $E_{sr}$  are considered, the peak associated with SVIA events is the lowest, while, if only those occurrences for which  $f_0 E_s > 5$  Mc/s are considered, the peak associated with SVIA events is the highest.

This finding is interpreted as implying that the proton energy spectrum giving rise to  $E_{sr}$  is harder during SVIA than at other times, and that the SVIA is caused by ionization at lower levels generated by the more energetic protons.

Theoretical calculations (Eather and Burrows 1966) have been carried out on the ionization,  $H\beta$  intensity and line profile, and cosmic radio noise absorption due to protons with various energy spectra. Comparison of the observed and theoretical line profiles indicates that 1–10 keV protons are responsible for the  $H\beta$ . It is found that  $10^7$  protons  $\text{cm}^{-2}\text{sec}^{-1}\text{sr}^{-1}$  with isotropic angular distribution and energy of 6 keV will produce 0.55 dB absorption at 27.6 Mc/s;  $10^4$  protons  $\text{cm}^{-2}\text{sec}^{-1}\text{sr}^{-1}$  at 100 keV will produce 1.1 dB absorption;  $4 \times 10^2$  protons  $\text{cm}^{-2}\text{sec}^{-1}\text{sr}^{-1}$  at 1000 keV will produce 1.3 dB absorption. Thus a hardening of the proton energy spectrum giving a flux of  $10^4$ – $10^5$  protons  $\text{cm}^{-2}\text{sec}^{-1}\text{sr}^{-1}$  at 100 keV is sufficient to explain all SVIA events. Such fluxes have been observed by rocket flights in the auroral zone (Davis, Berg, and Meredith 1960; McIlwain 1960; see Table 1).

The weak diffuse aurora associated with SVIA is not thought to be excited by protons. Although the intensity ratio  $I(\lambda 4709)/I(H\beta)$  increases with increasing proton energy, it is still only 0.18 for proton energies of 130 keV (Chamberlain 1961), while the observed ratio is invariably greater than unity in the diffuse aurora associated with SVIA. This then implies that there is some electron precipitation during typical SVIA events. This conclusion is confirmed by the sometimes patchy distribution of the luminosity in  $\lambda 4709$  and  $\lambda 5577$  as compared with the invariably very diffuse distribution of  $H\beta$ .

It is difficult to assess the relative importances of hardening of the proton and electron energy spectra from ground-based observations. Balloon altitude measurements should show enhanced X-ray fluxes during SVIA if hardening of the electron energy spectrum is important. The use of rockets offers the possibility of direct, *in situ*, measurement of the energy spectra.

#### IV. ACKNOWLEDGMENTS

The observations were carried out while one of us (R.H.E.) was a member of the Australian National Antarctic Research Expedition at Mawson during 1963. We should like to acknowledge the assistance of members of this expedition, especially Mr. D. Creighton, who kept the large amount of electronic equipment operational and gave invaluable assistance in many other ways. Ionospheric data were supplied by Mr. R. Schaeffer of the Ionospheric Prediction Service. We also thank Dr. K. M. Burrows of the University of New South Wales for valuable discussion and comments on the manuscript.

The latter part of this work was completed while one of us (R.H.E.) held a CSIRO Post-graduate Studentship at the University of New South Wales.

V. REFERENCES

- ANSARI, Z. A. (1963).—*Geophys. Inst., Univ. Alaska, Scient. Rep. No. 4, NSF Grant No. G144133.*
- APPLETON, E. (1954).—*J. Atmos. Terr. Phys.* **3**: 282.
- BARCUS, J. R. (1965).—*J. Geophys. Res.* **70**: 2135.
- BROWN, R. R. (1964a).—Kiruna Geophys. Observ., *Scient. Rep. Features of auroral energy spectrum inferred from observations of ionospheric absorption.*
- BROWN, R. R. (1964b).—Kiruna Geophys. Observ., *Scient. Rep. Day-night ratio of auroral absorption for breakup events.*
- BROWN, R. R., and BARCUS, J. R. (1963).—*J. Geophys. Res.* **68**: 4175.
- CAMPBELL, W. H., and LEINBACH, H. (1961).—*J. Geophys. Res.* **66**: 25.
- CHAMBERLAIN, J. W. (1961).—“*Physics of the Aurora and Airglow.*” (Academic Press: New York.)
- CHAPMAN, S., and LITTLE, C. G. (1957).—*J. Atmos. Terr. Phys.* **10**: 20.
- DAVIS, L. R., BERG, O. E., and MEREDITH, L. H. (1960).—“*Space Research I.*” p. 721. (North Holland: Amsterdam.)
- EATHER, R. H., and BURROWS, K.M. (1966).—*Excitation and ionization by auroral protons.* *Aust. J. Phys.* **19** (in press).
- EATHER, R. H., and JACKA, F. (1966).—*Aust. J. Phys.* **19**: 241.
- GUSTAFSSON, G. (1964).—*Planet. Space Sci.* **12**: 195.
- HEIKKILA, W. J., and PENDSTONE, S. R. (1961).—*Canad. J. Phys.* **39**: 1875.
- HOLT, C., LANDMARK, B., and LIED, F. (1961).—*J. Atmos. Terr. Phys.* **23**: 229.
- HOLT, O., and OMHOLT, A. (1962).—*J. Atmos. Terr. Phys.* **24**: 467.
- HULTQVIST, B. (1963a).—*Planet. Space Sci.* **11**: 371.
- HULTQVIST, B. (1963b).—*J. Atmos. Terr. Phys.* **25**: 225.
- HULTQVIST, B. (1964).—*Planet. Space Sci.* **12**: 579.
- LITTLE, C. G., and LEINBACH, H. (1959).—*Proc. Inst. Radio Engrs* **47**: 315.
- McDIARMID, I. B., and BUDZINSKI, E. E. (1964).—*Canad. J. Phys.* **42**: 2048.
- McDIARMID, I. B., ROSE, D. C., and BUDZINSKI, E. (1961).—“*Space Research II.*” p. 1194. (North Holland: Amsterdam.)
- McILWAIN, C. E. (1960).—*J. Geophys. Res.* **65**: 2727.
- MANN, L. G., BLOOM, S. D., and WEST JR., H. I. (1963).—“*Space Research III.*” p. 447. (North Holland: Amsterdam.)
- MEREDITH, L. H., DAVIS, L. R., HEPPNER, J. P., and BERG, O. E. (1958).—*IGY Rocket Rep. Ser. No. 1*, p. 169.
- OMHOLT, A. (1960).—*Proc. Electromagnetic Wave Propagation Symp.* 1957, p. 75.
- PARTHASARATHY, R., and BERKEY, F. T. (1965a).—*J. Geophys. Res.* **70**: 89.
- PARTHASARATHY, R., and BERKEY, F. T. (1965b).—*Radio Sci.* **69D**: 415.
- PARTHASARATHY, R., LERFALD, G. M., and LITTLE, C. G. (1963).—*J. Geophys. Res.* **68**: 3581.
- REES, M. H. (1964).—*Planet. Space Sci.* **11**: 1209.
- ZIAUDDIN, S. (1961).—*Nature* **191**: 1084.

APPENDIX I

*Multifrequency Absorption Measurements*

The absorption  $A$  of cosmic radio waves of frequency  $\omega$  is given by

$$A \propto \int_0^{\infty} \frac{N\nu}{\omega^2 + \nu^2} d\nu,$$

where  $N$  is the electron density,  $\nu$  the electron collision frequency, and  $h$  the height.

If the absorption is assumed to take place in a thin height interval, we can distinguish the following three possibilities:

$$\begin{aligned}\omega &\gg \nu \text{ then } A \propto 1/\omega^2, \\ \omega &\ll \nu \text{ then } A \text{ is independent of } \omega, \\ \omega &\sim \nu \text{ then } A \text{ depends on both } \nu \text{ and } \omega.\end{aligned}$$

To use multifrequency measurements to derive the height of the absorbing layer, the frequencies must be selected so that they are of the same order as the electron collision frequencies in the absorbing layer. Measurements in the region  $\omega \gg \nu$  give only a lower limit for the height (Parthasarathy, Lersfeld, and Little 1963).

## APPENDIX II

### *Time Differences in Intensity and Absorption Peaks*

The continuity equation for electrons may be written

$$dN/dt = q/(1+\lambda) - aN^2,$$

where  $N$  is the electron density,  $q$  the electron production rate,  $a$  the effective recombination coefficient, and  $\lambda$  the ratio of negative ion to free electron densities. Solving this equation we obtain

$$N = \frac{N_0\{aq/(1+\lambda)\}^{\frac{1}{2}} + \{q/(1+\lambda)\}\tanh[\{aq/(1+\lambda)\}^{\frac{1}{2}}.t]}{\{aq/(1+\lambda)\}^{\frac{1}{2}} + aN_0\tanh[\{aq/(1+\lambda)\}^{\frac{1}{2}}.t]},$$

where  $N_0$  is the electron density at  $t = 0$  and  $q$ ,  $\lambda$ , and  $a$  have been assumed constant. Note that  $N \rightarrow N_e = \{q/a(1+\lambda)\}^{\frac{1}{2}}$  as  $t \rightarrow \infty$ .

If, at  $t = 0$ , there is a step-function increase in  $q$ , the electron density will increase to the equilibrium value  $N_e$  as  $t \rightarrow \infty$ . After a time  $t_{90}$  given by

$$\tanh[\{aq/(1+\lambda)\}^{\frac{1}{2}}.t_{90}] = (N_0 - 0.9N_e)/(0.9N_0 - N_e),$$

the electron density will attain a value  $N(t_{90}) = 0.9N_e$ . If  $N_e \gg N_0$ ,

$$t_{90} \simeq 1.47\{(1+\lambda)/aq\}^{\frac{1}{2}} = 1.47/aN_e.$$

The greater the value of  $q$  (and hence  $N_e$ ) the shorter will be this time lag.

However, if, after a time interval less than  $t_{90}$  when  $N = N'$ ,  $q$  rapidly drops to zero (at  $t' = 0$ ),  $N$  will immediately decrease at a rate determined by  $dN/dt' = -aN'^2$ , that is,  $N = N'/(at'N' + 1)$ . The electron density will be reduced to the value  $N(t'_{90}) = \frac{1}{10}N'$  after a time  $t'_{90} = 9/aN'$ .

It is apparent that if there is a sudden increase, which is sustained, in the flux of ionizing radiation and hence in the auroral intensity (assuming the ratio of auroral intensity to electron production rate,  $I/q$ , to be constant) the increase in absorption will show a time lag. If the auroral intensity shows a short duration peak (with rapid recovery), this will be accompanied, without time lag, by an attenuated peak in absorption. If successive peaks in auroral intensity are separated by times short compared with the relaxation time constant  $t'_{90}$ , the absorption record will

smooth out the rapid fluctuations. If an auroral intensity level is maintained long enough for the electron density to reach its equilibrium value  $N_e$ , and then the flux of ionizing radiation is suddenly cut off, the electron density will decay to  $0.1N_e$  in a time  $t'_{90} = 9/aN_e$ . Note that both  $t_{90}$  and  $t'_{90}$  are proportional to  $1/N_e$ , and hence to  $1/A_e$ , where  $A_e$  is the equilibrium riometer absorption.

A further possibility may be of interest, namely, if  $q$  undergoes a smooth rise and fall through a maximum value  $q = \bar{q}$ , then  $N$  will pass through a maximum with a time delay  $\Delta t$  that may be estimated by the following method due to Appleton (1954).

$$\left(\frac{dN}{dt}\right)_{N=\max} = 0 = \left(\frac{dN}{dt}\right)_{q=\bar{q}} + \left(\frac{d^2N}{dt^2}\right)_{q=\bar{q}} \Delta t.$$

Since  $d^2N/dt^2 = -2aN dN/dt$ , we obtain

$$\Delta t = 1/2aN_{\bar{q}},$$

where  $N_{\bar{q}}$  is the value of  $N$  corresponding to  $q = \bar{q}$ .

### APPENDIX III

#### *Auroral Geometry Effects on the Intensity/Absorption Ratio*

Let the photometer and riometer fields of view be equal to unity. Assume that the intensity and absorption occur at close enough to the same height so that perspective effects may be neglected. Consider an aurora covering an area  $a$  of the field of view ( $a < 1$ ).

If the measured intensity at the photometer is  $I_m$ , then the actual auroral intensity is  $I_a = I_m/a$  within the area  $a$ .

Since  $A \propto N\nu$ , and  $N \propto q^{\frac{1}{2}}$  (see Appendix II), then, assuming  $I/q$  constant,

$$A \propto I_a^{\frac{1}{2}}.$$

If absorption takes place only in the area of the aurora, then we can show

$$A_a = -10 \log\{1 - (1 - 10^{-A/10})/a\},$$

where  $A_a$  is the absorption occurring in the aurora and  $A$  is the measured absorption. Thus we expect

$$A_a \propto I_a^{\frac{1}{2}}.$$

Whereas, if the absorption takes place over the whole field of view, we have

$$A \propto I_a^{\frac{1}{2}}.$$

